Computational Simulation of a wing in ground effect

K. MALTI[1], B. IMINE[1]

[1]Aeronautics and Propulsive Systems Laboratory. Faculté de Génie Mécanique Université des Sciences et de la Technologie D'Oran Mohamed BOUDIAF BP1505 El M'nouar 31000 Oran Algérie

Abstract –

The aim of this work is to present a numerical simulation of flow around a wing profile NACA0015 under the ground effect, A CFD software has been used to determine the aerodynamic performance of the wing for different angles of incidence. This study is subdivided in two main parts that consists in a numerical study in two-dimensional and another in three dimensional.

*For the 2D study were carried out by varying the angle of attack α(0°, -5° and -10°), and ground clearance(h/c) with values0,25, 0,35, 0,45,and flow velocity (V), with values 40m/s, 50m/s and 60m/s ,For this negative angle of attack (α) and a decreasing of the ground clearance (h/c), There was a slight increase in drag, while the lift decreases significantly. The study in 3D was calculated with positive angle of attack (0°, 2°, 4°, 6° and 8°), which gives an increase in lift and an increase in the pressure still at the intrados. When the wing is close to the ground, the vortices do not develop and the aerodynamic characteristics of the wing are similar to those of the profile. The Spalart-*Almaras turbulence *model was adopted for the investigation of complex flow around the profile.*

Comparison the results of our study with the experimental results of the predecessors are found a correlation.

Keyword :*ground effect, profile NACA0015, CFD, aerodynamic coefficients*

NOMENCLATURE

c chord length,

Cl coefficient of lift

Cd coefficient of drag

Cp coefficient of pressure

D drag force

H height of trailing edge above the ground,

L lift force

P static pressure

t Time

u mean velocity, m/s

μ dynamic viscosity

α angle of attack

δ_{ij} Kronecker symbol

I Introduction

During the first decades of the twentieth century; in the domain of automobile, aerodynamic research has been carried on the drag reduction to reach the performance of the vehicle speed peak. During the second half of this century, this development continued in the same direction, with reduction or reversal of the lift motor to increase their roll stability and running speed on a bend. During this century, manufacturers have resulted in the stability of some types of vehicles, without reducing drag, but rather maintaining it constant or even increasing it. Assuming truncated trailing edges, the rear axle is bearing on delimit, which also allows a better stability of vehicles (Fig. 1).

Fig.1. New Elise diffuser without intermediate ribs

In the case of a ground-effect aircraft; flight near the ground increases slightly the lift slope, which reduces the angle of incidence, the deflection and the drag caused by the lift. This reduction improves the smoothness of the vehicle and its fuel saving, thereby increasing its autonomy. The proximity to the ground creates a barrier to the downward flow of air, normally associated with the lift. The downward deflection is a function of the height; these effects are generally considered negligible when the flight is at a height that exceeds the span of the wing(Fig 2).

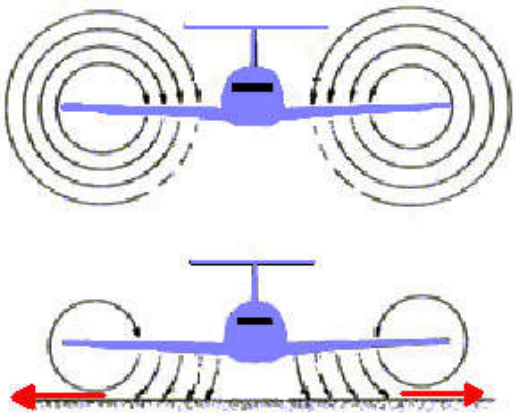

Fig.2. Vortex Movement Near Ground

First, the ground effect has been widely used for the benefit of the maritime domain; particularly decked catamarans active services, thereafter it was introduced in the field of aeronautics.

Hiromitsu Kawazoe; Shinji Morita [1], conducted a study on a triangular wing in ground effect. The model is tested in a wind tunnel. The purpose of this test is to examine the aerodynamic characteristics such as lift and drag. The results showed that the triangular wing is more efficient compared to other forms of wings.

H. Ibrahim Hebow in his thesis entitled 'entre bondary Interference layers on an Airfoil and flat plate [2] conducted an experimental study on a wing profile in ground effect, LK and K. Kliment Rokhsaz [3] present a study on a pair of vortices in ground effect, tested in a water tunnel. They concluded that the vortices undergo a rebound near the ground.

MH Djavareshkian, A. Esmaeli, A. Parsani(2010) [4] performed a numerical estimate with FLUENT for the wings with small fins near the ground. The results showed better aerodynamic performance at the fins with less turbulence as compared with that of the wing without fins

MH Djavareshkian, A. Parsania, Esmaeli A., and A. Ziaforoghi(2011) [5], in a comparison over several turbulence models of flow around a wing at different ground clearance and angle of attack, they found the reliability of the model Spalarts Almaras.

the flow characteristics over a symmetrical airfoil NACA0015 are studied experimentally in a low speed wind tunnel by ahmed an al.(2001)[7]. The pressure distribution on the airfoil surface was obtained, lift and drag forces were measured and mean velocity profiles were obtained over the surface, As a result, they obtained a higher values of lift coefficient are when the airfoil is close to the ground. Sayuti.

Syamsuar, E. B. Djatmiko, P. A. Wilson, Erwandi, Subchan.(2013) [8].present a study of The adaptive control system implemented on the Remote Control model Amphibian configuration to anticipate the porpoising effect during hydro planing on the longitudinal and lateral mode This control system also maintaining the ground effect on the 0.25 m altitude height to reduce the Pilot workloads.

Baddoo et al. (2020)[9] delved into research on the ground effect phenomenon, obtaining several exact solutions and elucidating the underlying physical mechanisms involved in ground effect. Jing Feng et al. (2022)[10] explored the ground effect phenomenon and its impact on the performance of three straight rectangular models by using a numerical solution (CFD). They applied the results to aircraft control and stability. Shi et al. (2022)[11] investigated the effect of the ground effect phenomenon on supersonic nozzle performance. They conducted a numerical analysis of the aerodynamic characteristics of a supersonic nozzle in the presence of ground effect

II.PHYSICAL MODEL

We chose an airfoil commonly used in aerospace application. It has been acknowledged NACA0015 profile belongs to traditional NACA four-digit series. The incidence α is defined as an angle between the direction of the undisturbed flow and the axis of symmetry of the profile. H is the distance between the ground and the lower surface, determined from the extreme point of the trailing edge. In the context of numerical study, it varies: The angle of attack α, the flow velocity V, the distance H to estimate the lift and drag coefficient (Figure 3.).

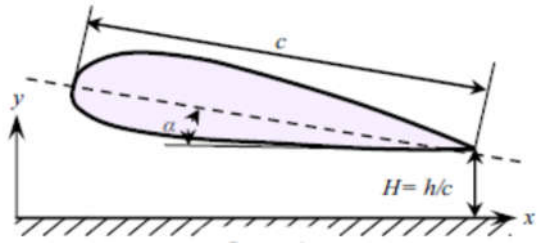

Fig. 3. Geometry of physical problem

III. THE EQUATION OF TRANSPORT AND MODEL TURBULENCE

The flow around the wing is considered turbulent. The general form of the transport equations can be written in cartesian coordinates as follows:

Continuity equation

$$\frac{\partial}{\partial xj}\left(\bar{\rho}\widetilde{U}_J\right) = 0 \ (1)$$

Movement conservation equation

$$\frac{\partial}{\partial xj}\left(\bar{\rho}\widetilde{U}_i\widetilde{U}_j\right) = \bar{\rho}g_i - \frac{\partial \bar{p}}{\partial x_i} - \frac{\partial}{\partial xj}(\bar{\rho}U''_iU''_j) + \frac{\partial}{\partial xj}\left[\mu\left(\frac{\partial \widetilde{U}_i}{\partial xj} + \frac{\partial \widetilde{U}_j}{\partial xi}\right) - \frac{2}{3}\bar{\mu}\frac{\partial \widetilde{U}_k}{\partial x_k}\delta_{ij}\right] (2)$$

The resolution was carried by the turbulence model "Spalart-allmaras"

$$\frac{\partial}{\partial t}(\rho\tilde{v}) + \frac{\partial}{\partial x_i}(\rho\tilde{v}u_i) = G_v + \frac{1}{\sigma\tilde{v}}\left[\frac{\partial}{\partial x_i}\left\{(\mu - \rho\tilde{v})\frac{\partial\tilde{v}}{\partial x_j}\right\} + G_{b2}\left(\frac{\partial\tilde{v}}{\partial x_j}\right)^2\right] - Y_v + S_{\tilde{v}} (3)$$

In this study the mesh was generated using GAMBIT and FLUENT was the solver employed in this CFD study. All experimental data in present research is from the thesis of H. Ibrahim Hebow; University of Aleppo (Syria) [2].

IV. GEOMETRY CREATION IN "GAMBIT"

The main emphasis was developing a grid that ensures resolutions in agreement with the available literature. Both treated geometric configurations are shown below.

IV. 1. Two dimensional simulations

The geometry considered is composed of four distinct surfaces and a NACA 0015profile. The Cord Length is 0.1m and the width is 0.02 m. The separation into four areas is to enable to refine the mesh without imposing a total number of items too high (Figure 4. 1 and fig. 4.2).

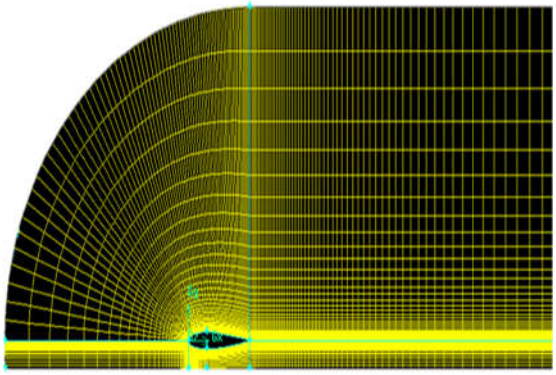

Fig. 4. 1. Mesh of the domain 2d case

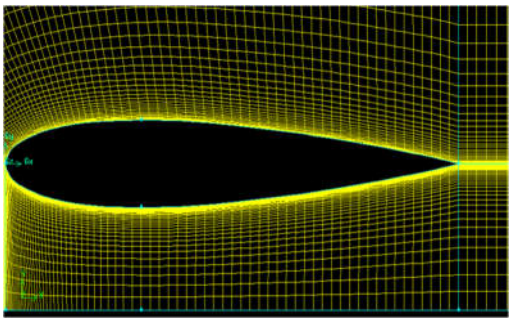

Fig. 4. 2. Mesh of the domain 2d case

IV.2. Three dimensional simulations

The most difficult areas are numerically grasped the lower surface and the wake of the profile. A very refined mesh is essential in these areas. The chosen dimensions allow carrying out a calculation to obtain the various characteristic values up to ten times the rope downstream of the model (Fig. 5.1 and Fig. 5.2). Initial conditions and boundary of the computational domain were chosen so as to reproduce the conditions of the experiment.

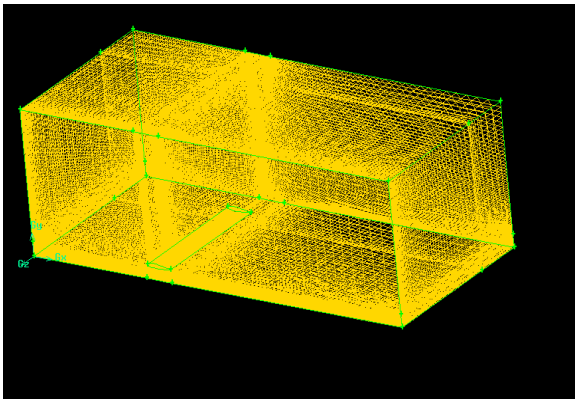

Fig.5.1. Mesh of the domain 3d case

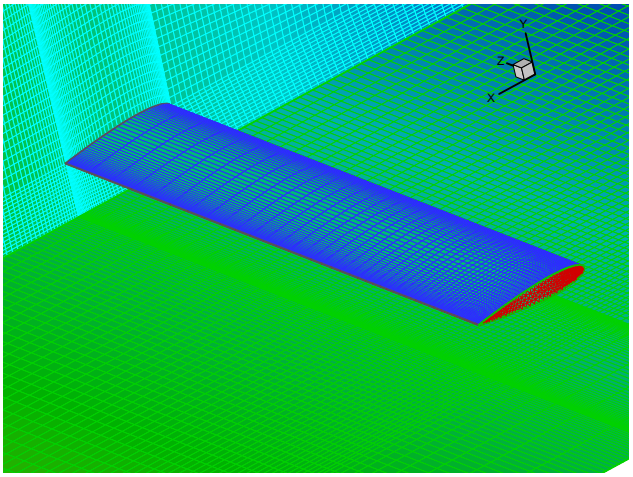

Fig. 5.2. Meshing around the wing

The boundary conditions imposed are:
At the inlet, velocity has been prescribed. At outlet, the pressure is fixed. Slip boundary conditions are used on upper walls of the domain and wall boundary conditions are used for airfoil surface and ground surface. (Fig. 6). A summary of the boundary conditions used are shown in (Fig. 6).

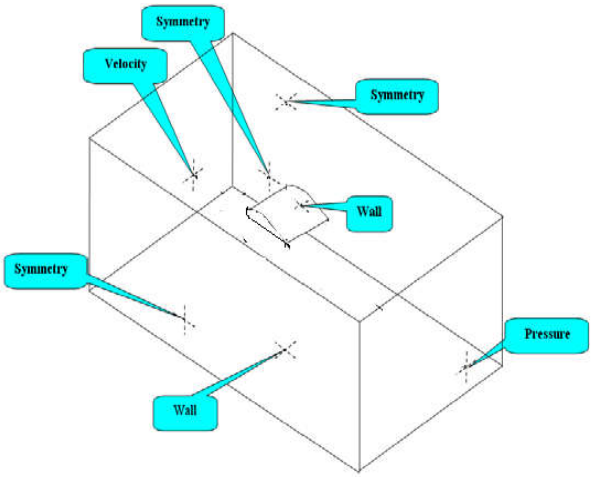

Fig.6. Representation of the boundary conditions in the 3d case

V. RESULTS

V.1. Correlation between the numerical and experimental study presented H.IBRAHIM study (2006). [2]

The graphs (Figs. 1 to 7. 7. 3) show the variation of the lift coefficient versus angle of attack and the ground clearance. it indicates the same pace for the graphs of the two areas (numerical and experimental). A slight difference should be noted between the two curves in the stall area.

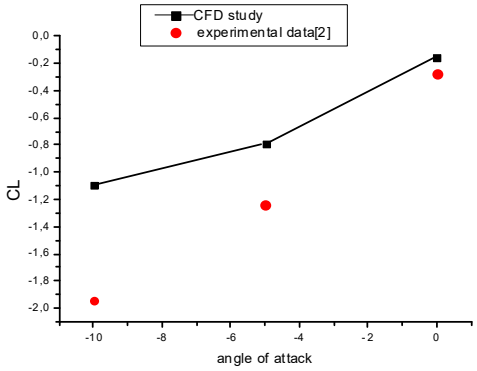

Fig. 7. Variations of the lift coefficient versus the angle of attack, at h / c = 0.25

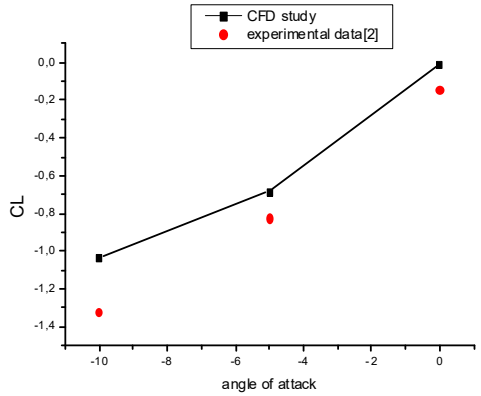

Fig.7. 2. Variations of the lift coefficient versus the angle of attack,at h / c = 0.35

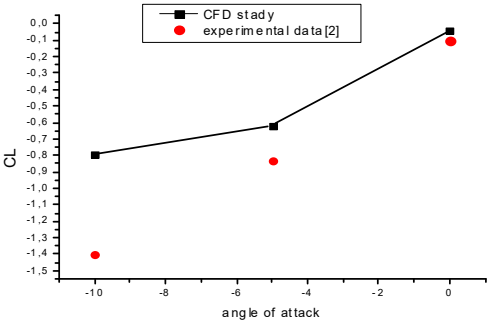

Fig.7. 3. Variations of the lift coefficient versus the angle of attack,at h / c = 0.45

The change in drag. (Figs 4 to 7. 7. 6.); Conformity between the graphs of the two studies is only partial; This is shown in the two graphs in a reduction of the drag coefficient versus the angle of attack α, but depending on the ground clearence 'h / c', this analogy exists only at α = -10 °

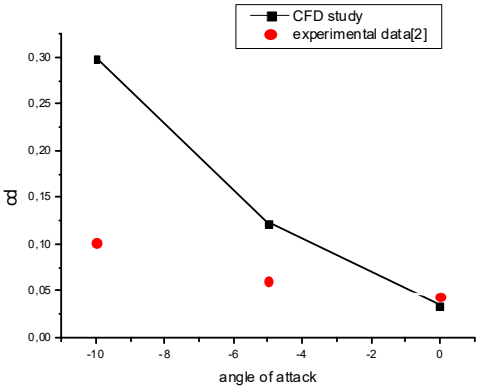

Fig. 7. 4. Variations of drag coefficient versus the angle of attack, at / c = 0.25

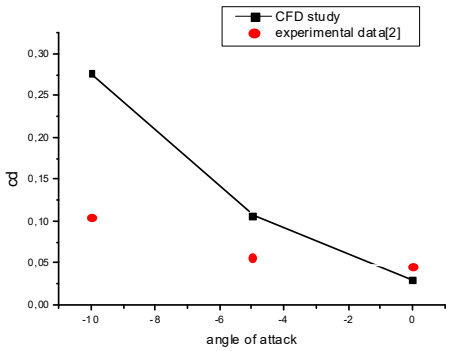

Fig. 7. 5. Variations of drag coefficient versus the angle of attack, h / c = 0.35

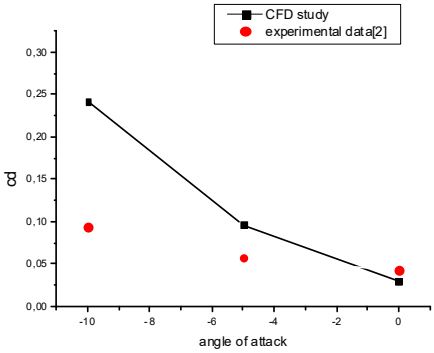

Fig. 7. 6. Variations of drag coefficient versus the angle of attack, h / c = 0.45

V. 2. Interpretation and discussion of results of pressure coefficient

The Figs (7. 7 ,7. 9) show the variation of pressure coefficients Cp over the surface of the pressure face with a ground clearance; H / C = 0.45, 0.35 and 0.25 and for the angles α1 = 0 °, α2 = - 5 ° and α3 = -10 °.At the pressure side, for V1 = 40m / s and α = 0 °; near the leading edge, there are three drop peaks, which indicate a variation of the pressure coefficient 'Cp' of -0.5 to -0.85. From the lowest peak occurs a gradual increase of 'Cp'. On the rope from 40% to 80%, a more prominent difference is observed in the curve h / c = 0.25, which is a larger depression. Á After this interval, the three curves merge. For α = -5 °, the pressure drop coefficient of the peaks are lower relative to those of α = 0 °. A fast increase of the pressure coefficient and we notice a lag between the curves; and for α =- 10 °, the general shape of the curves is the same, but with even stronger fall peaks

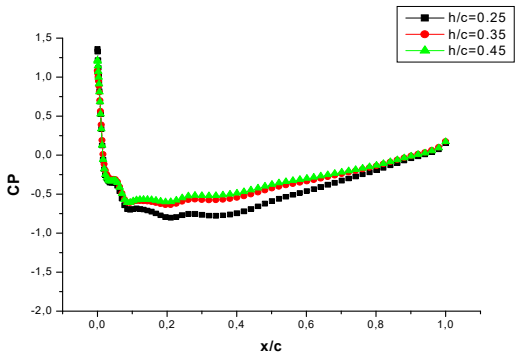

Fig. 7. 7. Variations of pressure coefficient Intrados (V= 40m/s et α= 0°)

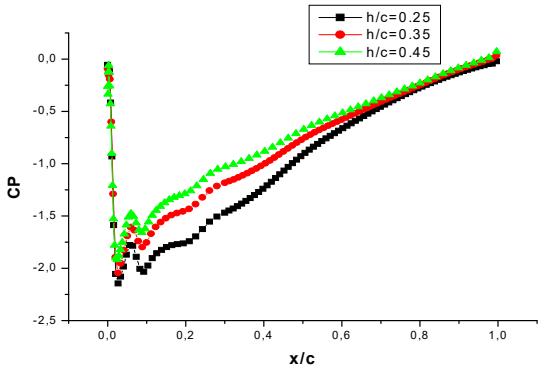

Fig. 7. 8. Variations of pressure coefficient Intrados (V= 40m/s et α= -5°)

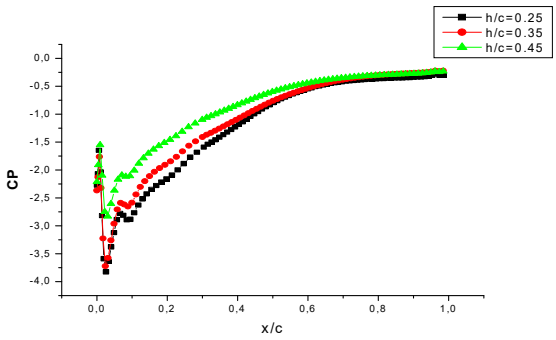

Fig. 7. 9. Variations of pressure coefficient Intrados (V= 40m/s et α= -10°)

.

The figure (7. 10) shows the pressure coefficient 'Cp' on the surface of the pressure face to H / C = 0.25 v = 40m / s v = 50m / s and v = 60m / s .We observed appearance of combined curves, indicating that the increase in speed does not affect the distribution of pressure on the pressure side.

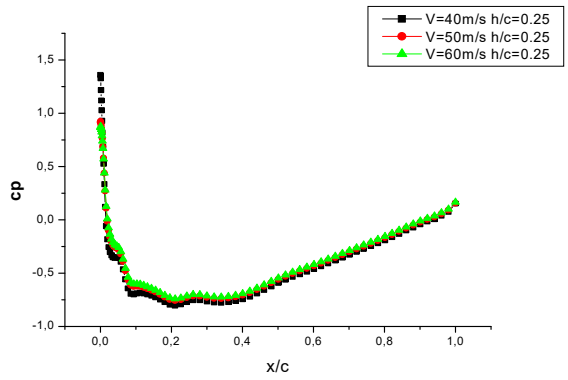

Fig. 7. 10. Variations of pressure coefficient Intrados at h/c=0.25 (V= 40m/s ; V= 50m/s ; V= 60m/s)

.

Figure (7. 11 to 7.15), show the variation of pressure coefficients Cp over the surface of the pressure face with a ground clearance; H / C = 0.45, 0.35, 0. 25, 0.2 and 0.1, for angles of attack α1 = 0 °, α2 = 2 °, α3 = 4 °, α4 =6 ° and α5 = 8 ° with the velocity V1 = 40m / s. By adopting an increase in angle α and decreasing ground clearance h / c = 0.45 h / c = 0.1, we observe an increase of the pressure coefficient and is noted also that the pressure coefficients are predominantly positive.

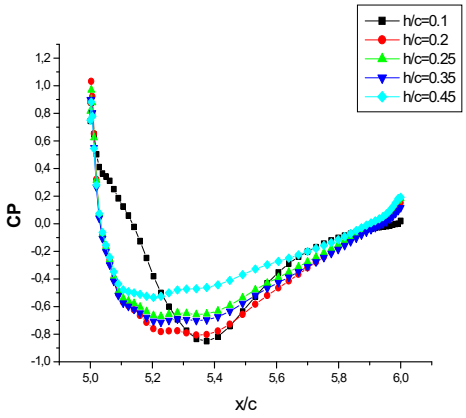

Fig. 7. 11. Variations of pressure coefficient Intrados (V= 40m/s et α=0°)

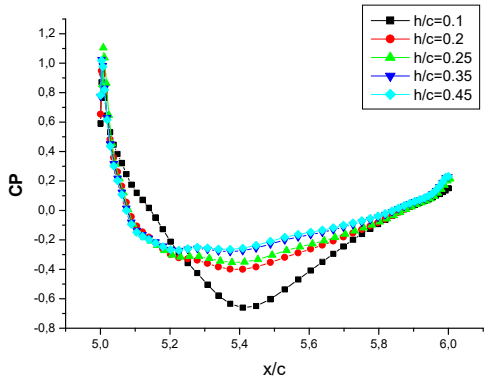

Fig. 7. 12. Variations of pressure coefficient Intrados (V= 40m/s et α= 2°)

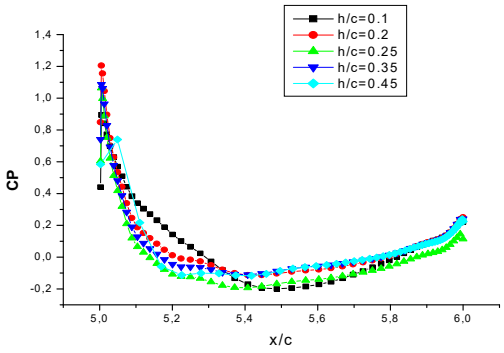

Fig. 7. 13. Variations of pressure coefficient Intrados (V= 40m/s et α= 4°)

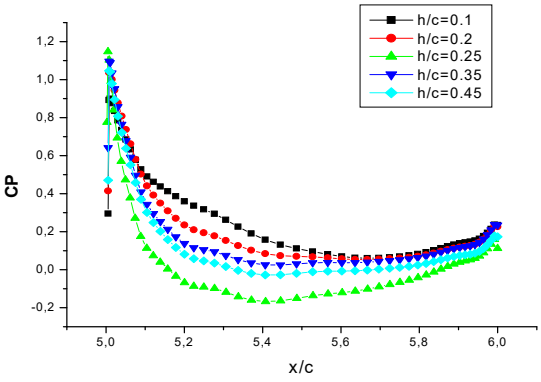

Fig. 7. 14. Variations of pressure coefficient Intrados (V= 40m/s et α= 6°)

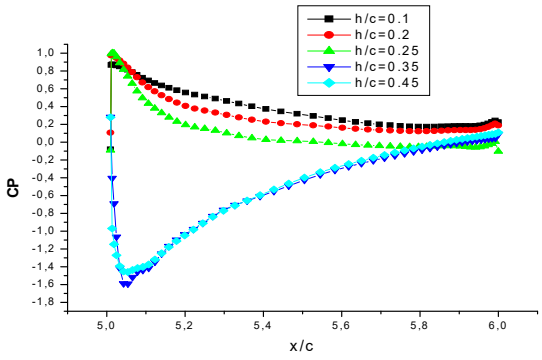

Fig. 7.15. Changes in pressure coefficient Intrados (V= 40m / s α = 8 °)

Figure (7. 16) shows the pressure coefficient 'Cp' on the surface of the pressure face to H / C = 0.25 v = 40m / s; v = 50m / s and v = 60m / s and α = 8 °. There is a slight difference of the curve v = 60m / s, indicating that the increase in speed does not have a great influence on the distribution of pressure on the pressure side.

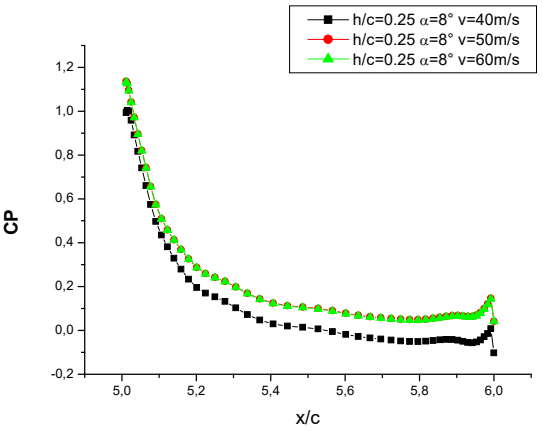

Fig. 7. 16. Variations of pressure coefficient Intrados (V_1= 40m/s,V= 50m/s, V= 60m/set α= 8°)

V.3. Interpretation and discussion of results the coefficient of drag and lift

For the study of the variation of the two coefficients (drag and lift), we proceed to change the angle α attack and ground clearance 'h / c' without changing the speed When the measurement of the angle of attack increases from 0 ° to -10 °, an increase in the drag coefficient 'Cd' is realized (Fig. 7. 17) and when the angle changes from 0 ° to 8 °, also an increase of the drag coefficient. When the ground clearance 'h / c' decreases from 0.45 to 0.1, the drag coefficient (Cd) increases slightly (fig. 7.18).

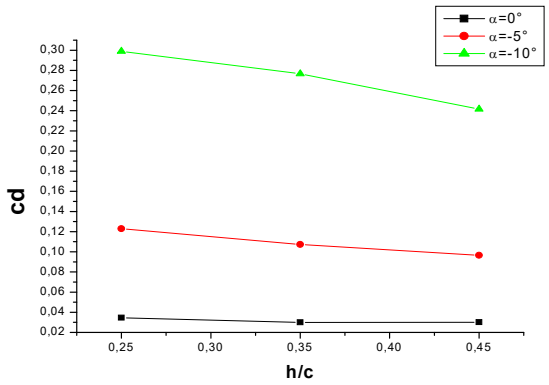

Fig. 7. 17. Variations in the coefficient of drag according to (h / c)

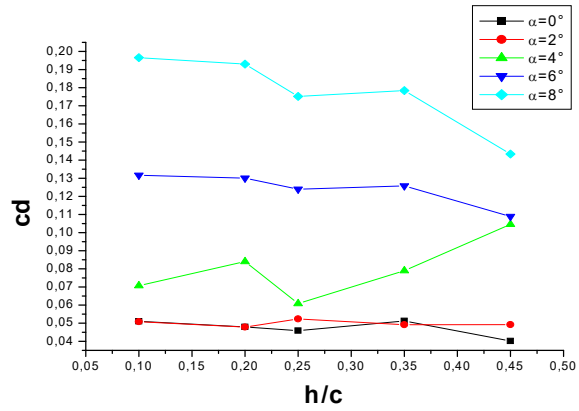

Fig. 7. 18. Variations in drag coefficient in function of (h / c)

When the measurement of the angle of attack increases from 0 ° to -10 ° was decreased lift coefficient 'CL' (Fig. 7. 19), when the angle changes from 0 ° to 8 ° the lift coefficient increases (Fig. 7. 20). When the ground clearance (h / c) decreases, the lift coefficient 'CL' increases.

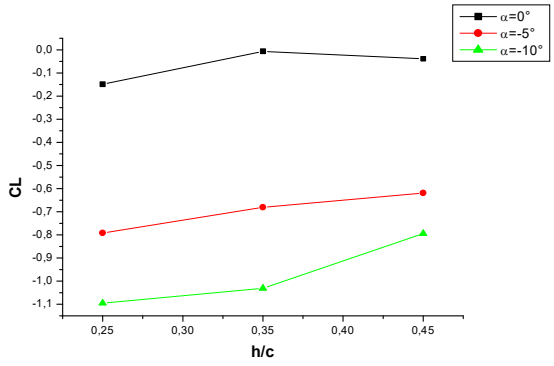

Fig. 7. 19Variations of the lift coefficient versus (h/c)

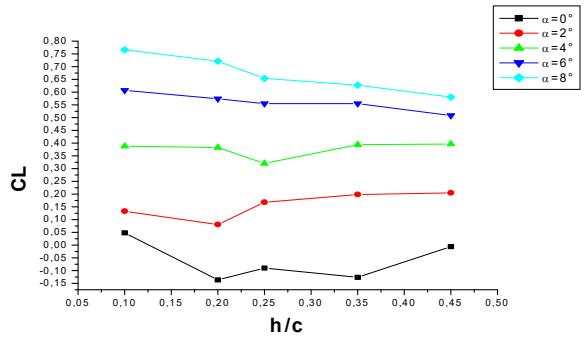

Fig. 7. 20. Variations of the lift coefficient versus (h/c)

VI.5. Trajectory of the flow pathlines

The effect seen in Figures 8.1 to 8.5est said winding cone shaped (Vortex); said 'vortex' for incidence α = 8 °, these vortices are more spread by reducing the ground clearance 'h / c'. This spreading generates a decrease of induced drag.

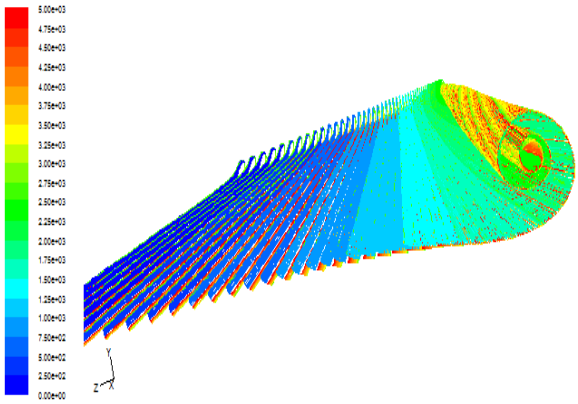

Fig. 8.1. The flow of attack 8 ° angle, h / c = 0.45 °

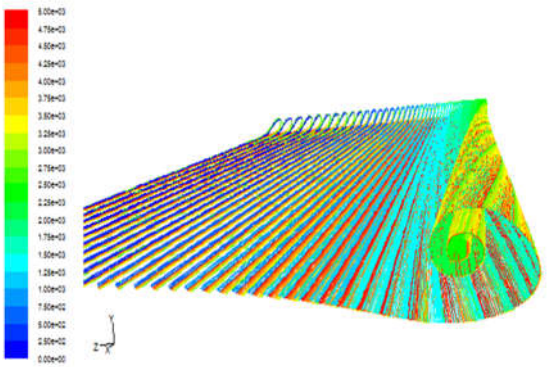

Fig. 8.2. the flow angle 8 ° and h / c = 0.35

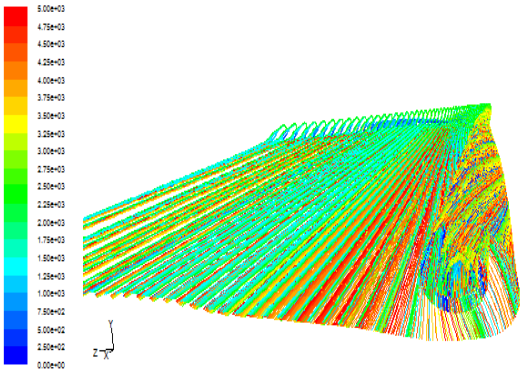

Fig. 8.3. The flow angle 8 ° and h / c = 0.25

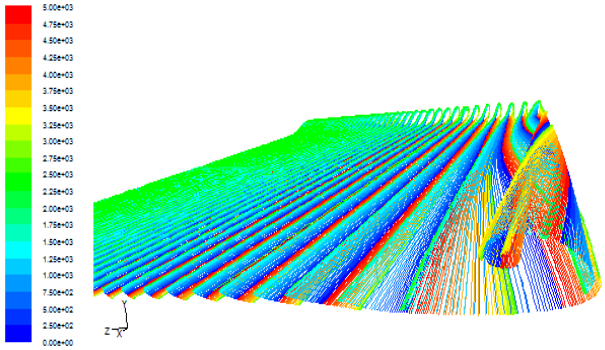

Fig. 8.4. The flow angle 8 ° and h / c = 0.2

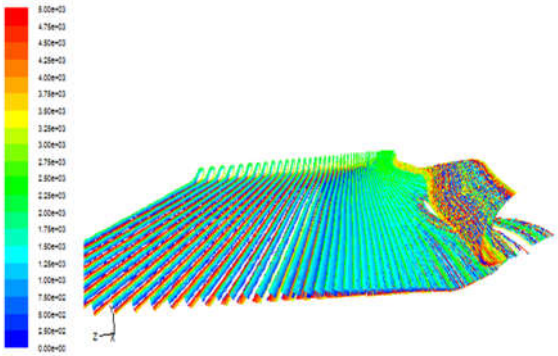

Fig. 8.5. The flow angle 8 ° and h / c = 0.1

VIII. CONCLUSIONS

For study the performance of a wing with profile NACA 0015 in ground effect, a detailed numerical investigation was carried out using FLUENT CFD code with the Spalart-Allmaras turbulence model. For this treatment, the parameters used are: The ground clearance, angle of attack, speed (40m / s, 50m / s and 60m / s). In this numerical study result the following conclusions: The decrease of ground clearance (h / c) and the angle of attack, causing a depression to the pressure side. Depression is explained by the circulation of the fluid in the passage divergent-convergent caused by the form between the

ground and the underside. The movement of fluid through this passage is in accordance with the Venturi phenomenon. The pressure on the pressure side increases for low values of the charge of the ground (h / c) and gradually as the angle of incidence increases, by the suction against the ground clearance does not show a significant variation. For low values of the guard ground (h / c) and for negative angles of incidence (α); the boundary layers of the soil and the lower surface may coalesce, producing a loss of dynamism in the flow and consequently an increase in drag (Cd). . The boundary layer separation occurs in the case of a low angle (10 °) The comparison between the experimental and numerical fields, gives a fairly good correlation

REFERENCES

[1] Hiromitsu Kawazoe, Shinji Morita, (2004). 'Ground Effect on the Dynamic Characteristics of a Wing-rock Delta Wing' tottery university, American Institute of Aeronautics and Astronautics,(AIAA).

[2] IBRAHIM. H, (2006). Interférences between boundary layers on an Airfoil and a flate plate. Thesis master degree in Mechanical Engineering. Aleppo University. 123p.

[3] Kliment L. K. et Rokhsaz K. (2008). 'Experimental Investigation of Pairs of Vortex Filaments in Ground Effect' university Wichita. American Institute of Aeronautics and Astronautics,(AIAA), Vol. 45, No. 2 , pp. 622-629

[4] Djavareshkian M.H., Esmaeli A., Parsani A., (2010). 'Aerodynamics of smart flap underground effect'University of Mashhad', Aerospace Science and Technology, Vol 15, No. 8,pp. 642-652

[5] Djavareshkian M. H.,.Parsania A., Esmaeli A., and Ziaforoghi A. (2011) 'Investigation of Turbulence Model to Simulation of Ground Effect in 2D and 3D Cases', International Conference on Fluid Dynamics and Thermodynamics, Dubai, January 25-27.

[6] Forrester T. Johnson, Edward N. Tinoco and Jong Yu N., 'Thirty years of development and application of CFD at Boeing Commercial Airplanes, Seattle',16th AIAA Computational Fluid Dynamics Conference

[7] M.R. Ahmed a, S.D. Sharma b (2001)'An investigation on the aerodynamics of a symmetrical airfoil in ground effect, Aeronautics R&D Board, Ministry of Defense, Govt .of India, under project No. Aero/RD-134/100/10/2000-2001/1108'

[8] *Sayuti Syamsuar, E. B. Djatmiko, P. A. Wilson, - Erwandi, - Subchan,* 'The Flight Performance Criteria for Adaptive Control Design During Hydro Planing and Ground Effect Altitude of Wing In Surface Effect-Craft';(2013) international, review of mechanical engineering,(IREME)Vol 6, No 5

[9] Peter J. Baddo Melike Kurt Lorna J. Ayton Keith W. Moored(2020) 'exact solutions of the ground effect'Published online by Cambridge University Pres

[10] Jingfeng X., Lei, S., Huang, J., & Jingcheng, F. (2022). 'Parameter study on lateral moments of banked wings in ground effect.' Chinese Journal of Aeronautics

[11] Shi, Y., Chen, L., Chen, P., Yang, Q., Shi, Y., & Yang, H. (2022). Numerical study on aerodynamic characteristics of supersonic nozzle in presence ofground effect. Journal of Physics: Conference Series,Publisher: IOP Publishing Pages, 012013.